JOURNAL OF CATALYSIS **168,** 217–234 (1997)
ARTICLE NO. CA971652

The Interaction of Nitrogen with the (111) Surface of Iron at Low and at Elevated Pressures

I. Alstrup,* I. Chorkendorff,† and S. Ullmann*

*Haldor Topsøe Research Laboratories, Nymøllevej 55, DK-2800 Lyngby, Denmark; and †Center for Atomic-scale Material Physics (CAMP), Physics Department, Technical University of Denmark, Building 307, DK-2800 Lyngby, Denmark

Received November 18, 1996; revised February 4, 1997; accepted February 5, 1997

New adsorption results have been obtained for the N_2/Fe(111) system using partial and total pressures from 10^{-4} to 500 Torr and temperatures in the range 393–578 K. They show that the initial, dissociative chemisorption probability is, within the accuracy of the measurements, independent of the gas temperature in contrast to molecular beam results corresponding to much higher gas molecule energies. This result suggests that the dissociative chemisorption of N_2 proceeds at thermal energies via a precursor-mediated process rather than a direct, activated process. It also confirms the validity of the adsorption results of F. Bozso, G. Ertl, M. Grunze, and M. Weiss (*J. Catal.* 49, 18, 1977) obtained using low-pressure exposures. However, the appearances of a 5×5 LEED pattern and TPD spectra with two peaks, a sharp one and a broader one, show that a new chemisorption state is created during exposures at nitrogen pressures $\geq$50 Torr and temperatures above 570 K. The stability of the new state increases strongly with the concentration of surface nitrogen and disappears rapidly when the concentration decreases below a critical value. It is then transformed into the well-known $(3\sqrt{3} \times 3\sqrt{3})$R30° surface structure, which also disappears rapidly below a lower critical surface concentration. After adsorption saturation at ~0.85 monolayer (ML) the coverage can be increased to ~1.1 ML by segregation. Bulk thermodynamic estimates indicate that the 5×5 surface state can be formed under industrial ammonia synthesis conditions. However, the presence of strongly bound hydrogen containing surface species may prevent its formation.

1. INTRODUCTION

The ammonia synthesis reaction on iron catalysts is industrially one of the most important catalytic processes and scientifically one of the most thoroughly investigated catalytic reactions. The pioneering, extensive and systematic surface science studies by Ertl and co-workers of the interactions of reactants and products with iron single-crystal surfaces and of the influence of the important promoter, potassium, have been and continue to be an important model for other surface science studies of catalytic reactions. These studies, which have been discussed in a number of reviews (1–6), inspired and formed the experimental basis for attempts by Stoltze and Nørskov (7, 8) and by Bowker *et al.* (9) to establish a detailed description of the process in terms of microkinetic models with the parameters determined on the basis of the surface science results. The reasonable agreement between the conversions measured under industrial conditions and those calculated by means of the microkinetic models indicated that despite the fact that the surface science studies were made on single crystals at pressures not exceeding 4×10^{-4} Torr (1 Torr = 133 Pa), they may be used to obtain an understanding of the industrial process taking place on the catalyst surface at pressures of 100 bar or more.

The initial sticking probability of nitrogen is observed to be about 20 times higher on Fe(111) (10) than on Fe(100) (10) and about 60 times higher than on Fe(110) (11), and from investigations of the activation of singly and doubly promoted iron catalysts it is concluded that the active catalyst surface consists predominantly of Fe(111) planes (12, 13). This means that nitrogen chemisorption results obtained for catalysts should be qualitatively similar to those obtained for the Fe(111) surface. The results of Ertl and co-workers showed that the activation energy of the dissociative chemisorption of N_2 on the clean Fe(111) surface is close to zero (10). The results obtained by Emmett and Brunauer (14) and by Scholten *et al.* (15) showed, on the other hand, that N_2 chemisorption on iron catalysts is an activated process. In the latter work an activation energy of 96 kJ/mol was obtained at surface coverages in the range 0.25–0.70 of a monolayer. Molecular beam studies by Rettner and Stein (16) revealed that the initial sticking probability of N_2 chemisorption of Fe(111) depends strongly on the energy of the impinging nitrogen molecules. In a recent temperature-programmed adsorption and desorption study of nitrogen on iron catalysts (17) it was concluded that the adsorption rate on the singly promoted catalyst was orders of magnitude lower than can be extrapolated from the single-crystal results of Ertl and co-workers (10). These catalyst results and single-crystal beam studies have called into question the applicability of the adsorption results of Ertl and co-workers (10) to the modeling of

0021-9517/97 $25.00

the kinetics of the ammonia synthesis reaction (18, 19). It is common practice when studying adsorption or reaction in ultrahigh vacuum (UHV) systems to limit the pressure during exposures of the sample to the milli-Torr region or lower in order to avoid jeopardizing the UHV conditions of the system. In the adsorption experiments of Ertl and colleagues (10) the N_2 pressure never exceeded 4×10^{-4} Torr. This means, however, that a possible gas temperature dependence of the chemisorption probability may not be correctly reflected in the results. At low pressures, where the mean free path of the gas molecules is not small compared to the distance between the sample and the chamber walls, which are kept at room temperature, the gas molecules hitting the sample will not be in thermal equilibrium with the sample at elevated temperatures. Studies of the activated chemisorption of CH_4 on nickel surfaces may be mentioned as a striking example where erroneous results were obtained because of the use of low pressures during exposures (20–23). In this case it was clearly demonstrated that the dissociative chemisorption of CH_4 proceeds via a direct process on Ni(111) (24) and Ni(100) (25). In the present work we have investigated the effect of using elevated pressures during N_2 exposures of a Fe(111) surface in the temperature range 393–809 K on the adsorption and segregation curves and on temperature-programmed desorption (TPD) spectra. The total pressure and the nitrogen partial pressure have been varied in the range 0.0001–500 Torr. The nitrogen experiments have been supplemented by potassium and hydrogen sulfide adsorption experiments with the purpose of establishing reliable translations of X-ray photoelectron spectroscopy (XPS) areas into coverages. We have in addition performed a temperature-programmed adsorption experiment to throw more light on the very low dissociative nitrogen sticking probability obtained for a singly promoted iron catalyst in the above-mentioned catalyst experiment (17).

2. EXPERIMENTAL

The experiments were carried out in an UHV system with two UHV chambers. One chamber is equipped with facilities for XPS and TPD and the second with an ion sputter gun, low-energy electron diffraction (LEED) and connection to a gas inlet system. The XPS facility is essentially identical to the standard VG ESCA 3 spectrometer. A Balzers quadrupole mass spectrometer, Type QMG 420 C, with a differentially pumped gold-plated shroud around the ionizer, was used for the TPD experiments with the sample surface facing the entrance aperture (2 mm diameter) of the shroud at a distance of ~1 mm. LEED patterns were recorded by means of reverse view LEED optics, Model RVL 6-120, from Princeton Research Instruments Inc. Very pure gases, nitrogen and argon (Alphagaz, >99.9999%), were used. The gases were further purified by passage through an activated nickel catalyst. The nitrogen exposures were made by rapidly backfilling the second chamber to the desired pressure, which was measured with a capacitance pressure gauge (MKS baratron). Most of the exposures were made with pure nitrogen but some were made with a mixture of nitrogen and argon to obtain a low nitrogen partial pressure and a high total pressure.

2.1. Cleaning of the Crystal

The iron crystal slab (diameter, 6 mm; thickness, 1 mm) with (111) surface orientation (±0.5°) was, before introduction into the UHV system, exposed to a flow of pure hydrogen at 1 bar and 1116 K for almost 1100 h. The temperature of the crystal was measured with a chromel/alumel thermocouple spotwelded to the backside of the crystal. After very many cycles of argon ion sputtering at ~1000 and at 500 K and subsequent brief annealing at 650 K the coverage of impurities was finally below the limit of detectability (~0.01 monolayer (ML)) (1 ML = 7.05×10^{18} atoms m^{-2} for Fe(111)). To minimize contamination from dissociation of background CO the crystal was always kept at temperatures above or equal to 440 K, except in cases where experiments were carried out at lower temperatures.

2.2. Estimation of Coverages

The amount of nitrogen left on the Fe(111) surface after evacuation subsequent to adsorption, segregation, or TPD experiments was monitored by means of XPS using Al$K\alpha$ radiation from a dual anode. The pass energy of the analyzer was 100 eV in all recordings. The XPS peak intensity ratio of the N 1*s* to the Fe 3*p* peak, $R_{N,Fe}$, was used as a measure of the nitrogen surface concentration. The areas of the XPS peaks were determined after subtraction of a nonlinear background using the algorithm suggested by Shirley (26). Although this method is based on a model which has been shown not to be physically correct (27) it gives satisfactory results when used for a limited energy region covering one peak (28). By consistently using the same region in all the area determinations for the same peak the ratio $R_{N,Fe}$ gives a reasonably accurate, relative measure of the nitrogen coverage. However, a reliable translation of the ratio $R_{N,Fe}$ into a nitrogen surface coverage is not easily obtained. The nitrogen adsorption structures on Fe(111) have not been solved. In our preliminary report of some of the present adsorption results (29) the surface nitrogen concentration was estimated from the $R_{N,Fe}$ ratio by using the previously determined relation between carbon coverage on the Ni(100) surface and the XPS peak intensity ratio, $R_{C,Ni}$, of the C 1*s* to the Ni 3*p* peak. For our apparatus and configuration it was found that $\theta_C/R_{C,Ni}$ is equal to ca. 12.7 ML (30) based on the fact that the C saturation coverage is known to be 0.5 ML for Ni(100) (23).

A value for $\theta_N/R_{N,Fe}$ was then obtained by scaling $\theta_C/R_{C,Ni}$ using photoionization cross sections calculated by Scofield (31), corrected for slightly different asymmetry parameters (Reilman *et al.* (32)), the atom density ratio of iron to nickel (0.927), and the monolayer atom ratio of Fe(111) to Ni(100) (7.05/16.1). We take advantage of the observation of Castle and West (33) that the energy dependence of the transmission function of our VG ESCA 3 energy analyzer is to a good approximation equal to the reciprocal of the energy dependence of the effective attenuation length of the photoelectrons, so they cancel out. The result of this estimate was $\theta_N/R_{N,Fe} \approx 10.8$ ML. The fact that the coverages obtained using this estimate are significantly higher than those reported by Ertl and co-workers (10) and that the highest coverage calculated was surprisingly high, ca. 1.4 ML (obtained after long time exposure to 50 Torr N_2 at 800 K), makes it highly desirable to obtain a more direct calibration of the XPS ratio. We have therefore looked for other Fe(111) adsorption systems for which information about coverages is available. Only for potassium and sulfur on Fe(111) have we found determinations of coverages reported. Lee *et al.* (34) studied adsorption of K on the (110), (100), and (111) surfaces of iron by means of LEED, Auger electron spectroscopy (AES), TPD, and work function measurements. In the case of Fe(111) a 3×3 structure was seen by LEED at fairly low coverages. It was suggested that this structure corresponds to a K coverage of 1/9 ML. The saturation coverages were then found to be 5.8×10^{14} K atoms/cm^2, almost the same as found for the other surfaces by other methods. Müller *et al.* (35) determined sulfur coverages on Fe(111) by means of quantitative AES and also by calibrating the AES measurements by using the fact that a coverage of 0.5 ML is well established for the c(2×2)S structure on Fe(100) (36) and obtained the same result by both methods. The result obtained corresponds to about 1 ML sulfur at saturation. We have established a new calibration of our XPS measurements by performing K and S adsorption experiments, as described below, and utilizing the above-mentioned coverage estimates (34, 35).

2.3. Adsorption of K and S

K was evaporated onto the clean Fe(111) surface at 288 K from a well-outgassed SAES getter source at a distance of 25 mm from the surface. Various K coverages were obtained by annealing the crystal at different temperatures and times after K deposition. A range of S coverages was obtained by exposing the clean Fe(111) surface at 450 K to H_2S for various lengths of time from a doser consisting of a plate with a 2-μm aperture and a tube with an inner diameter of 3.5 mm and a length of 100 mm. The H_2S pressure behind the aperture was 5 Torr. For both adsorbates the formation of adsorption-induced surface structures were looked for by means of LEED.

2.4. Near Surface Nitrogen Saturation of Crystal

Ertl and colleagues (10) observed that nitrogen can migrate from the surface into the bulk at temperatures above about 500 K. To derive correct sticking probabilities from surface coverage measurements at higher temperatures it is necessary to minimize this migration. Ertl and co-workers (10) attempted a near surface saturation by exposing the crystal to 4×10^{-4} Torr N_2 at 600 K for a long time before cleaning the surface by argon ion sputtering. Also in the present work a presaturation procedure was used, but much higher N_2 pressures were used and in most cases also much higher temperatures.

In most of the chemisorption or segregation experiments reported below the crystal was exposed to nitrogen at 50 or 500 Torr for 30 or 60 min at 809 K. The high-temperature exposures were always terminated by rapidly cooling the crystal down to 440 K while maintaining the nitrogen pressure. However, it turned out, as demonstrated below, that for very long adsorption exposures at higher temperatures a significant contribution to the coverage may come from segregation. In such cases less severe saturation conditions have been used; i.e., some long adsorption exposures have been made after nitrogen saturation exposure at 50 Torr, 578 K for 60 min. Also TPD spectra are strongly influenced by the severity of the presaturation procedure and indeed by the entire prehistory of the sample if bulk nitrogen is left from previous experiments. To obtain well-defined TPD results two series of TPD experiments were performed based on nitrogen exposures of 50 and 500 Torr, respectively, at different temperatures in the range 485–809 K with the crystal being emptied of bulk nitrogen between the experiments. The crystal was heated linearly from 440 to 948 K at a rate of 2 K/s after which desorption was continued at constant temperature, 948 K, until the desorption rate was negligible.

2.5. Nitrogen Adsorption Procedure

Before each series of adsorption experiments the near surface region of the crystal was partly saturated by exposing the crystal at high temperature to 50 or 500 Torr nitrogen and cooling down in nitrogen as described above. The surface was subsequently cleaned by argon ion bombardment at 440 K in about 10 min followed by a brief annealing at 624 K. Usually no impurities could be detected after this procedure. However, sometimes it was necessary to repeat the cleaning procedure to obtain an oxygen-free surface. Between the experiments the crystal was always kept at 440 K in order to minimize the accumulation of oxygen on the surface due to dissociation of CO from the very low background ($<5 \times 10^{-11}$ Torr). The exposures were made by heating the crystal to the desired temperature and rapidly backfilling the chamber to the selected exposure pressure. This procedure could be completed in about 10 s.

The exposure times used were larger than or equal to 2 min in order to keep the exposure uncertainty reasonably low.

3. RESULTS

3.1. K and S Adsorption

In agreement with Ref. (37) sharp third-order spots were obtained after 1 min K deposition followed by annealing at about 700 K for ca. 2 min. However, the determination of the area of the K 2*p* XPS peak is rather uncertain partly because of the weak signal due to the low coverage (1/9 ML) and partly because the spectrum is contaminated by a "ghost" peak due to a Fe 3*p* peak generated by the unwanted, weak Mg$K\alpha$ radiation from the dual anode. The area of the K 2*p* peak was determined after subtracting the spectrum of the clean Fe(111) surface. An example of a K 2*p* spectrum with the clean Fe(111) surface spectrum superimposed is shown in Fig. 1. The mean value of five determinations of the ratio, $R_{K,Fe}$, of the areas of the K 2*p* and the Fe 3*p* peak for slightly different annealing conditions, but corresponding to equally sharp 3×3 LEED patterns, gives $\theta_N/R_{N,Fe} \approx 7.6$. However, the spread in the values of the ratio is approximately $\pm 30\%$.

The sulfur chemisorption results are shown in Fig. 2. The rate of chemisorption is seen to be approximately constant up to a fairly high coverage ($\sim$0.75 ML), indicating a precursor mechanism. The mean value of the area ratio, $R_{S,Fe}$, of the S 2*p* and the Fe 3*p* peaks obtained in the saturation range of exposures corresponds to $\theta_N/R_{N,Fe} \approx 7.3$. The largest deviation is about 8% and only 4 of 19 determinations deviate more than 4%. Thus the ratio corresponding to sulfur saturation is determined fairly accurately and is used in the following for the translation of XPS peak area ratios into coverages assuming that sulfur saturation corresponds to 1 ML coverage. This is consistent with the fact that a sharp 1×1 LEED pattern is seen after sulfur saturation.

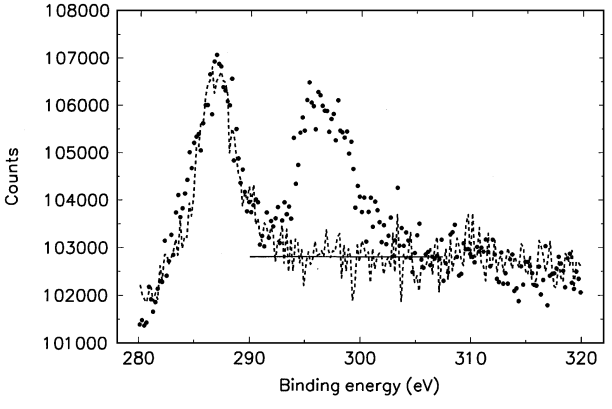

FIG. 1. Superposition of XPS spectra of the K 2*p* region for Fe(111) with (●) and without (- - -) K. The peak at 287 eV is a Fe 3*p* peak generated by unwanted Mg$K\alpha$ radiation.

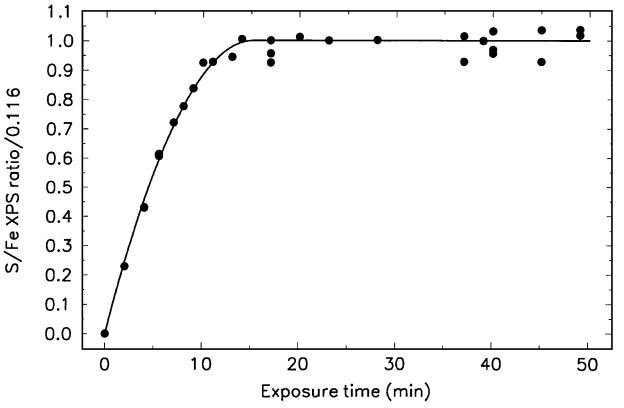

FIG. 2. S coverage as a function of H_2S exposure time at 450 K.

It is seen that the sulfur calibration is consistent with the K chemisorption results but gives coverages significantly lower than that used in our preliminary report (29).

3.2. Nitrogen Adsorption

The nitrogen adsorption results obtained at 485 K for a variety of partial and total pressures in the range 0.001–500 Torr are plotted in Fig. 3 versus the nitrogen exposure in ML units, i.e., twice the number of N_2 molecules hitting the surface during exposure divided by the number of surface iron atoms (7.05×10^{18} m^{-2}). Because of the large range of exposures covered a logarithmic (base 10) exposure scale is used. It is seen that the coverages measured at exposures below $\sim 10^8$ ML are independent of the total gas pressure: results obtained using gas mixtures of nitrogen and argon with total pressures of 1 and 10 Torr are not significantly different from results obtained with pure nitrogen at pressures of 0.001 and 0.1 Torr. It may be concluded

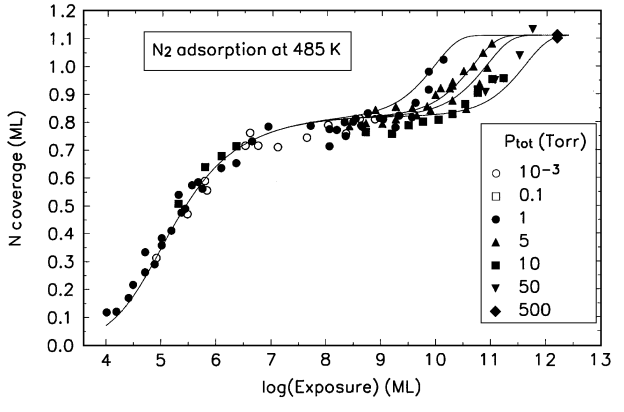

FIG. 3. Dissociative chemisorption of N_2 on Fe(111) at 485 K after saturation and cleaning of the surface. Results obtained with different total pressures during exposure in the range 10^{-3}–500 Torr are shown with different symbols. Curves represent Langmurian model calculations of adsorption plus segregation.

that at a surface temperature of 485 K and an effective gas temperature ≤485 K the dissociative sticking probability of nitrogen is independent of the gas temperature. It is seen in Fig. 3 that the coverage does not increase in the exposure range 10^7–10^8 ML but increases again at higher exposures, and that the adsorption curve depends strongly on the pressure in this high-exposure range. This behavior is obviously caused by segregation. Increasing the pressure seems to displace the upbending of the adsorption curve toward higher exposures, suggesting that the decisive parameter is the exposure time, i.e., that segregation of bulk nitrogen contributes to the measured coverage at long exposure times. Separate segregation experiments, reported below, confirm that the apparent increase of the sticking probability in the high-exposure range takes place at exposure times for which significant segregation is observed on the clean surface in vacuum after the same saturation procedure. Thus by including segregation this effect can easily be modeled as shown by the solid lines in Fig. 3. Similar observations of the influence of segregation were made also by adsorption experiments at higher surface temperatures. Adsorption results obtained at the temperatures 393, 439, 485, 531, and 578 K are plottet in Fig. 4. Results influenced by segregation are not included. To make it possible to distinguish results at different temperatures those obtained at 393 and 439 K are displaced down 0.2 and 0.1 ML, respectively and those obtained at 531 and 578 K are displaced up 0.1 and 0.2 ML, respectively; i.e., the scale of the vertical axis corresponds to the results obtained at 478 K. At the lower surface temperatures (393–440 K) a final coverage of ∼0.75 ML is obtained at the highest exposures, while a somewhat higher final coverage (∼0.85 ML) is obtained at

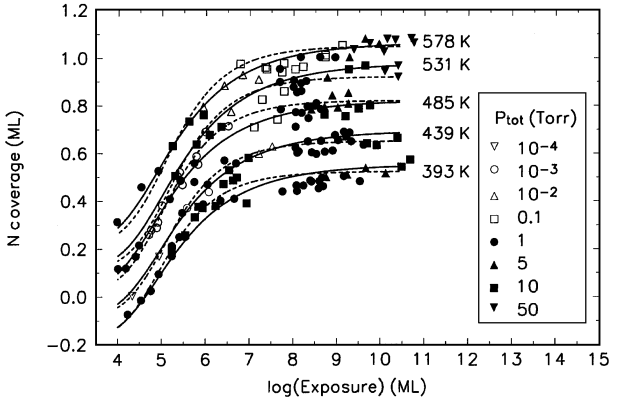

FIG. 4. Dissociative chemisorption of N_2 on Fe(111) after saturation and cleaning of the surface. Results obtained with different total pressures during exposure in the range 10^{-4}–50 Torr are shown with different symbols. Adsorption temperatures: 393, 439, 485, 531, and 578 K. Curves represent model calculations with third (---)- and fourth (—)-order dependence on concentration of free sites. Results for one temperature are offset vertically by 0.1 ML from the results of the next lower temperature. The coverage scale corresponds to the 485 K results. The model parameters are shown in Table 1.

TABLE 1

Parameters of Langmuir-Type Adsorption Model with Third- and Fourth-Order Dependence on Free Sites Concentration

T (K)	Saturation coverage (ML)	Initial sticking coefficient
393	0.72–0.75	8.3–10.0×10^{-6}
439	0.75–0.79	6.4–8.6×10^{-6}
485	0.82–0.83	8.3–12.8×10^{-6}
531	0.82–0.88	5.6–7.0×10^{-6}
578	0.85–0.86	7.2–12.5×10^{-6}

surface temperatures in the range 485–625 K. In Fig. 4, at each of the temperatures the adsorption results are compared with a simple Langmuir type adsorption model, i.e.,

$$\frac{d\theta_N}{dx} = s_0\left(1 - \frac{\theta_N}{\theta_{N,s}}\right)^n, \qquad [1]$$

where θ_N is the N coverage, x is the exposure, s_0 is the initial dissociative sticking probability, $\theta_{N,s}$ is the saturation coverage, and the exponent n can be interpreted as the number of free sites in an ensemble of minimum size which can dissociate N_2 on Fe(111). Various values of n have been tested. The values used for the curves in Fig. 4 are 3 (broken lines) and 4 (solid lines), which give better overall agreement than other integer values. The corresponding results obtained for the sticking probability and $\theta_{N,s}$ at the various temperatures are shown in Table 1. It is seen that the models give reasonable descriptions of the results obtained above 440 K, while at 393 and 439 K large, nonrandom deviations from the model curves are seen after short exposures at higher pressures. These deviations are believed to be due to an insufficient annealing after sputter cleaning. Due to the high pressure used during the presaturation procedure it was necessary to keep the annealing time short to avoid segregation. The adsorption results obtained just after sputtering and annealing deviates most from the curve while subsequent results obtained without intermediate sputter cleaning are closer to the curve.

3.3. Nitrogen Segregation

The segregation results obtained at 508, 531, 554, 578, 601, 624, and 647 K by monitoring the nitrogen coverage by XPS after exposing the crystal at 809 K to 50 Torr nitrogen for 30 min, cooling down in nitrogen, and cleaning the surface by argon ion sputtering are shown in Fig. 5. Similar results were obtained at 485, 531, 578, and 670 K after exposing the crystal at 809 K to 500 Torr nitrogen for 60 min, cooling down in nitrogen, and cleaning the surface by argon sputtering. The following simple segregation rate expression based on a first-order dependence on free sites

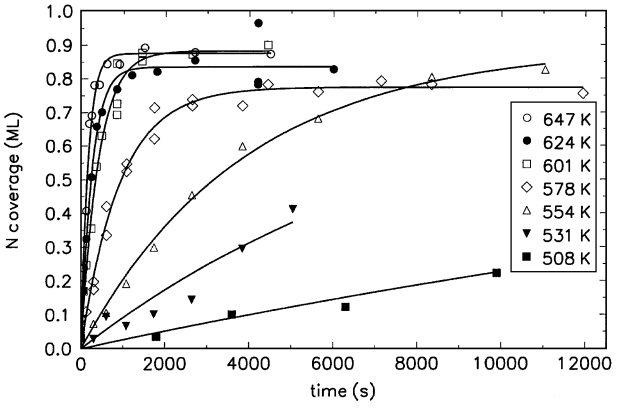

FIG. 5. Nitrogen segregation on Fe(111) after 50 Torr, 30 min saturation at 809 K, cooling in N_2, and cleaning of the surface. Segregation temperatures: 508, 531, 554, 578, 601, 624, and 647 K. Curves represent model calculations. The model parameters are shown in Table 2.

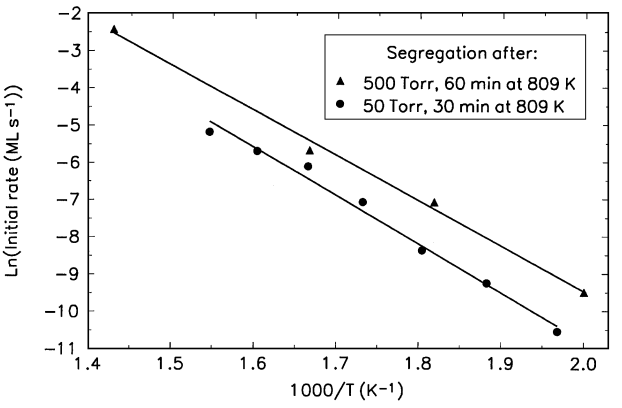

FIG. 6. Arrhenius plot of initial segregation rates after 50 Torr, 30 min and 500 Torr, 60 min saturation at 809 K, cooling in N_2, and cleaning of the surface.

was fitted to the results,

$$r_{\text{seg}} = k_{\text{s}}\left(1 - \frac{\theta_{\text{N}}}{\theta_{\text{N,seg}}}\right), \qquad [2]$$

where $\theta_{\text{N,seg}}$ is the segregation–saturation coverage and k_{s} the initial segregation rate. The parameters, $\theta_{\text{N,seg}}$ and k_{s}, of the curves plotted in Fig. 5 are shown in Table 2. An Arrhenius plot of the initial rate, k_{s}, is shown in Fig. 6. The slope of the regression line corresponds to an activation energy of 108 ± 5 kJ mol^{-1}. Initial segregation rates obtained after the 809 K, 500 Torr, 60 min nitrogen exposure are also shown in Fig. 6. In this case the saturation coverage increased to 1.05 ML and the slope of the regression line in Fig. 7 corresponds to an activation energy of 101 ± 5 kJ mol^{-1}.

The effect of different saturation procedures is shown in Fig. 7, where 578 K segregation results were obtained after three different 60 min exposures: (a) 809 K, 500 Torr; (b) 809 K, 50 Torr; (c) 578 K, 50 Torr with subsequent cooling down in nitrogen and sputter cleaning of the surface. Also segregation curves based on expression [2] are shown.

TABLE 2

Initial Segregation Rate and Saturation Coverage after 30 min 50 Torr N_2 Exposure at 809 K

T (K)	Saturation coverage (ML)	Initial rate (ML s^{-1})
508	0.87	2.6×10^{-5}
531	0.87	9.4×10^{-5}
554	0.89	2.3×10^{-4}
578	0.77	8.4×10^{-4}
601	0.88	2.2×10^{-3}
624	0.83	3.3×10^{-3}
647	0.87	5.6×10^{-3}

The parameters of the three segregation curves are shown in Table 3. It is seen that the initial segregation rate is increased by a factor of 3 when the pressure during exposure is increased by a factor of 10 and by a factor of about 16 when the exposure temperature is increased from 578 to 809 K.

In separate experiments it was demonstrated directly that it is possible to increase the coverage substantially by subsequent segregation after adsorption saturation has been reached. The results of such an experiment are also shown in Fig. 7. The crystal was first exposed at 809 K to 500 Torr nitrogen for 60 min and after sputter cleaning adsorption saturation, 0.85 ML, was reached by exposing the clean surface at 485 K to 50 Torr nitrogen for 4 min, i.e., an exposure corresponding to ca. 1×10^{10} ML. The nitrogen was then pumped out and the temperature was raised to 578 K. It is seen that segregation increased the coverage by ca 25% and that most of the increase took place in the first 7 min.

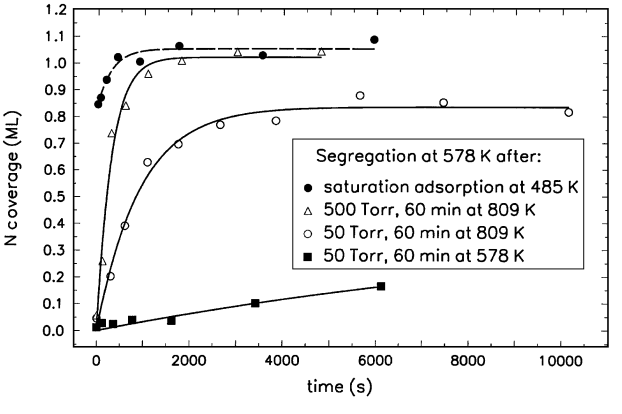

FIG. 7. Nitrogen segregation at 578 K after three different 60 min saturation exposures, 500 Torr, 809 K (△), 50 Torr, 809 K (○), and 50 Torr, 578 K (■), and after saturation adsorption at 485 K (●).

TABLE 3

Initial Segregation Rate and Saturation Coverage at 578 K after 60 min 500 or 50 Torr N_2 Exposure at 578 or 809 K

Exposure			
N_2 pressure (Torr)	T (K)	Saturation coverage (ML)	Initial rate (ML s^{-1})
500	809	1.0	2.2×10^{-3}
50	809	0.81	7.4×10^{-4}
50	578	0.47	4.7×10^{-5}

3.4. Simulation of a Catalyst Adsorption Experiment

Recently it was shown (17) that when a singly promoted iron catalyst is heated at a rate of 5 K/min from about 140 to about 350 K in a stream of nitrogen at a partial pressure of ca. 3 Torr the dissociative sticking probability calculated from the nitrogen partial pressure change is exceedingly small. This seems to indicate a strong difference between a Fe(111) single-crystal surface and the catalyst iron surface with respect to nitrogen adsorption. We have simulated the catalyst experiment by exposing the clean Fe(111) surface to a nitrogen pressure of 3 Torr while heating the crystal from 140 to 350 K. At the latter temperature the gas was pumped out and the crystal cooled down. The nitrogen coverage was determined by XPS to be about 0.65 ML. The sticking probability was subsequently determined by exposing the crystal to 5 Torr of nitrogen at 350 K. The exposure was interrupted after 10, 24, 44, and 74 min and the nitrogen coverage was determined by XPS. The maximum change in coverage was 0.085 ML obtained for an exposure of 7.2×10^9 ML, i.e., corresponding to a sticking probability of $\sim 1.2 \times 10^{-11}$. This is an upper limit because further exposures gave slightly lower coverages. This sticking probability is of the same order of magnitude as can be calculated from the nitrogen pressure change in the catalyst experiment. The experiment shows that a significant part of the nitrogen molecules adsorbed on the crystal at low temperatures are not desorbed during the temperature rise but are dissociated and stay on the surface as atoms causing the dramatic decrease in sticking probability.

3.5. LEED

The LEED observations by Ertl and co-workers (10) revealed the formation of a series of nitrogen-induced surface structures of Fe(111) dependent on the temperature and the nitrogen coverage. The sequence of structures observed was a 3×3 structure formed in the temperature range 410–470 K at relatively low coverages, and at increasing coverage a $(\sqrt{19} \times \sqrt{19})$R23.4° structure followed by a $(\sqrt{21} \times \sqrt{21})$R10.9° and a $(3\sqrt{3} \times 3\sqrt{3})$R30° structure. In addition they also observed the formation of a 2×2 structure when the crystal was kept at 610 K under vacuum for about 30 min after presaturation and surface cleaning. In the present experiments we had no difficulties in obtaining the 3×3 and the $(3\sqrt{3} \times 3\sqrt{3})$R30° structures. The 3×3 structure (Fig. 8a) could easily be formed at temperatures above ~440 K at coverages in the range 0.4–0.6 ML. At higher temperatures and usually also higher coverages the $(3\sqrt{3} \times 3\sqrt{3})$R30° structure was formed (Fig. 8b). However, at even higher coverages and temperatures (≥580 K) a new 5×5 structure appeared. This structure seems to be fully developed by a high exposure, e.g., 200 Torr in 30 min at 809 K, followed by cooling down in nitrogen at a brief anneal at 670 K (Fig. 8c). It should be emphasized that there is no simple relation between the surface structure and the coverage measured by XPS. Thus the 3×3, the $(3\sqrt{3} \times 3\sqrt{3})$R30°, and the 5×5 structures have been observed for coverages in the ranges 0.3–0.6, 0.7–1.1, and 0.85–1.3 ML respectively. In a number of stepwise, partial desorption experiments in UHV after very high exposures the same sequence of structures was always seen:

$$5 \times 5 \Rightarrow \left(3\sqrt{3} \times 3\sqrt{3}\right)\mathrm{R30}^\circ \Rightarrow 3 \times 3$$

We have not made special attempts to obtain the above-mentioned intermediate structures, $(\sqrt{19} \times \sqrt{19})$R23.4° and $(\sqrt{21} \times \sqrt{21})$R10.9°, and they did not appear probably because they are not stable under the conditions of our LEED experiments.

The details of one typical heat treatment sequence are as follows:

After the crystal with an initial coverage of 0.13 ML nitrogen had been presaturated by a 30 min exposure at 809 K to 260 Torr nitrogen and cooled down in nitrogen to 440 K for 30 min, a weak 5×5 pattern and a strong, diffuse background were seen. The XPS peak areas corresponded to a coverage of 1.35 ML. The crystal was then heated at 670 K for 2 min, reducing the coverage to about 1.3 ML and resulting in a sharp 5×5 LEED pattern and a low background. A subsequent 10 min heating at 670 K did not change the LEED pattern. The crystal was then heated in 1 min steps at temperatures that were increased by about 9 K at each step. The 5×5 pattern remained clearly visible after 10 steps ending at 763 K. Also after a subsequent 60 min heating at 670 K and another 1 min heating at 772 K the 5×5 structure could still be seen, but the $(3\sqrt{3} \times 3\sqrt{3})$R30° structure began to appear after the next 1 min heating at 781 K. Further heating for 3 min at 781 K brought the coverage down to about 1.06 ML and sharpened the $(3\sqrt{3} \times 3\sqrt{3})$R30° pattern considerably. After four more 1 min steps, the last at 809 K, the $(3\sqrt{3} \times 3\sqrt{3})$R30° became very weak and a 3×3 pattern appeared. After another 1 min heating at 818 K the 3×3 was sharp with little background. The coverage was now 0.54 ML. This sequence is illustrated in Fig. 9.

The 2×2 structure seen by Ertl and co-workers (10) after heating the presaturated crystal with an initially clean

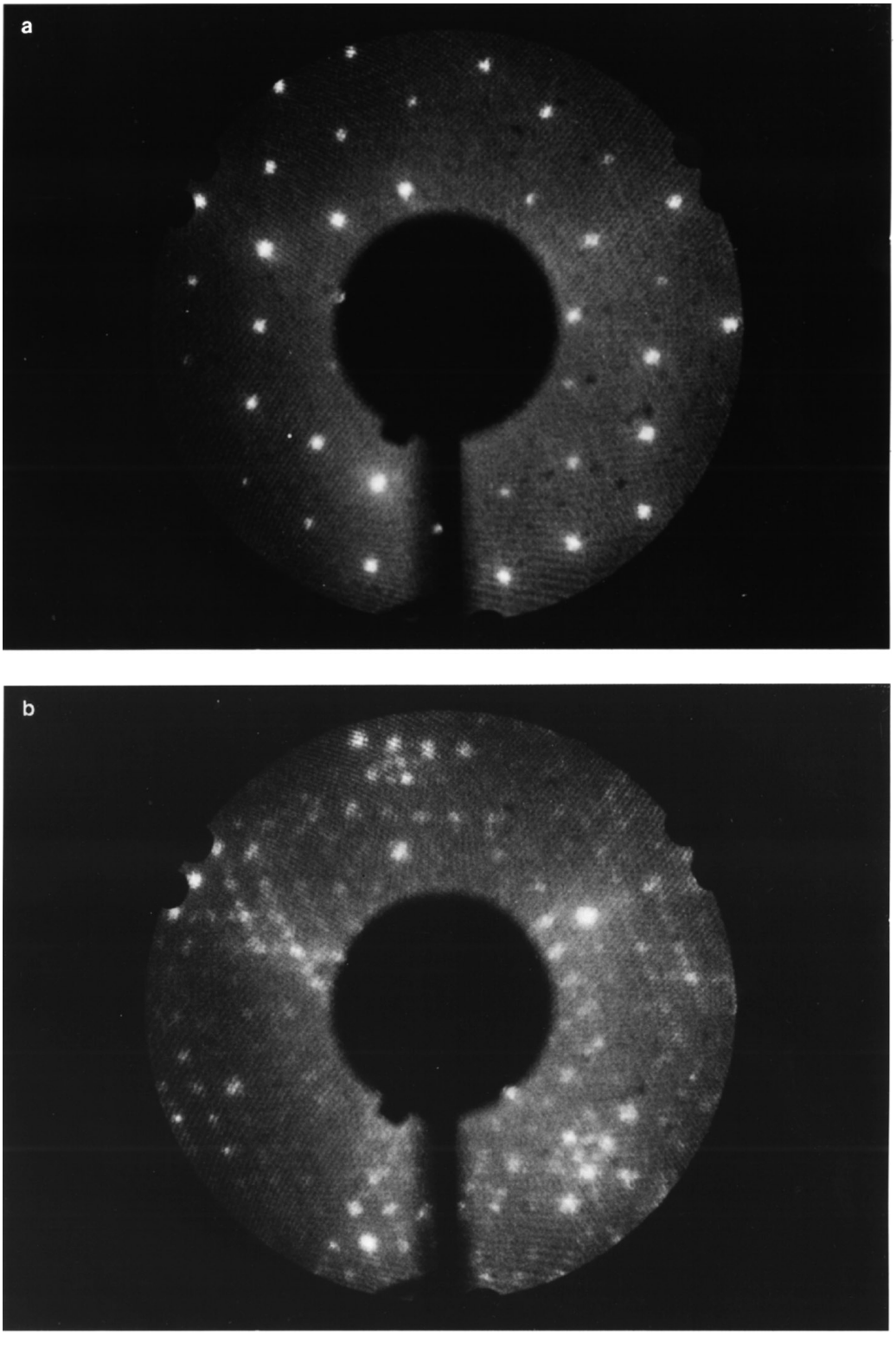

FIG. 8. LEED patterns obtained using an electron beam energy of 42 eV. (a) 3×3 structure obtained after 260 Torr, 30 min exposure at 809 K, cooling in N_2 plus 90 min step heat treatments (see Fig. 9). Coverage ~0.54 ML. (b) $(3\sqrt{3} \times 3\sqrt{3})R30^\circ$ structure obtained after 260 Torr, 30 min exposure at 809 K, cooling in N_2 plus 85 min step heat treatments (see Fig. 9). Coverage ~1.06 ML. (c) 5×5 structure obtained after 50 Torr, 60 min exposure at 800 K and cooling in N_2. Coverage ~0.96 ML. (d) 6×6 structure obtained after 50 Torr, 60 min exposure at 809 K and cooling in N_2. Coverage ~0.70 ML.

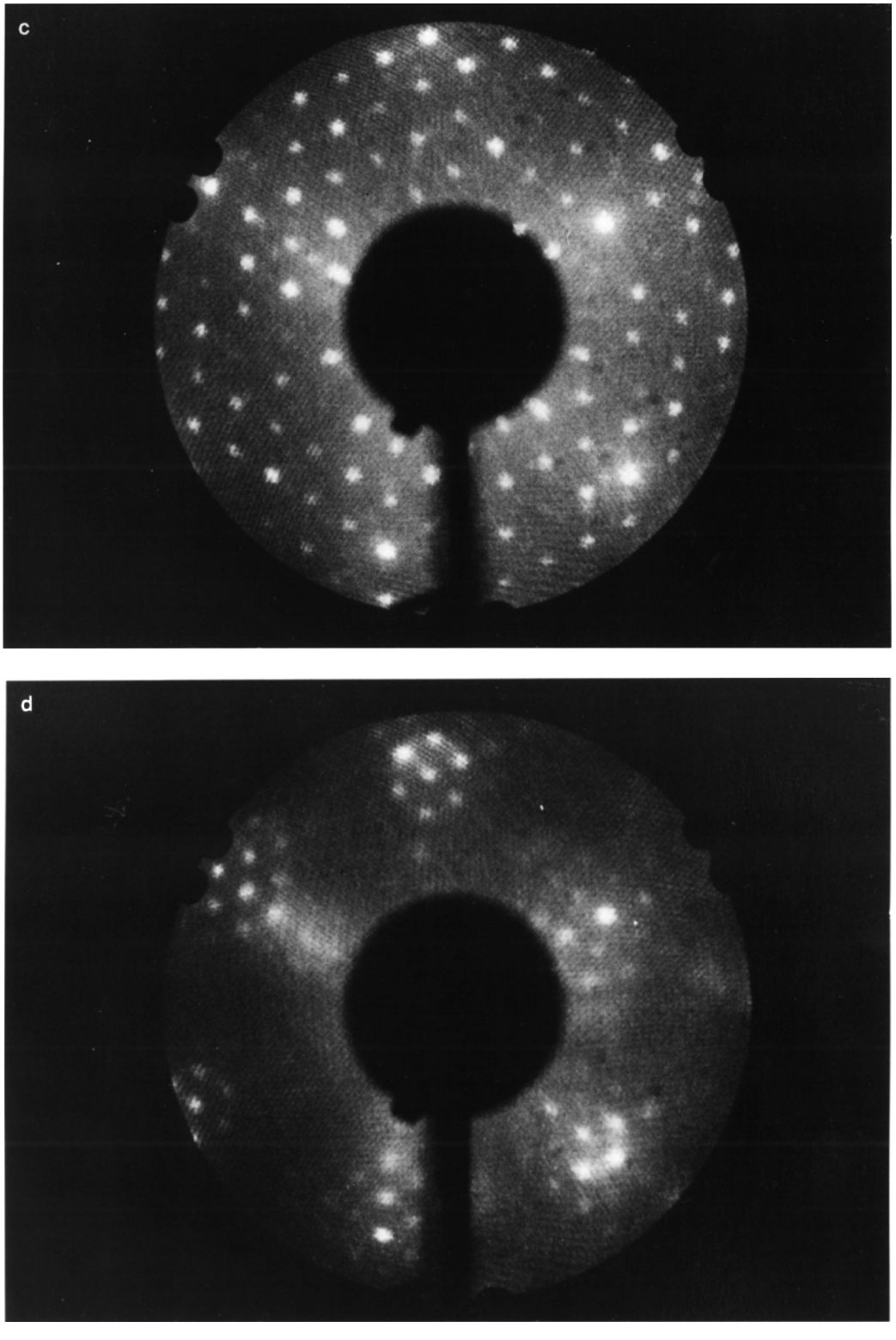

FIG. 8—*Continued*

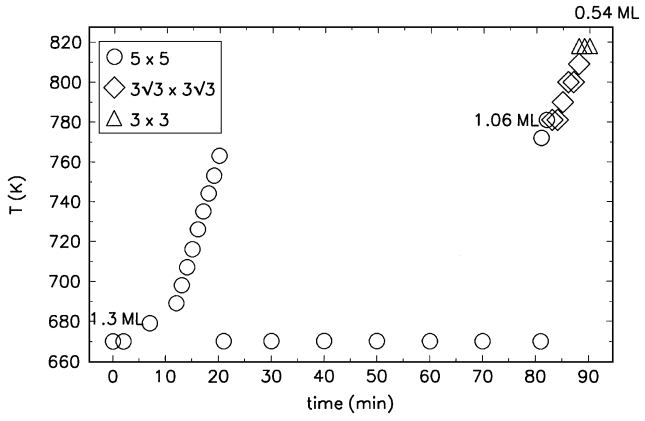

FIG. 9. LEED pattern changes during stepwise heating after 260 Torr, 30 min saturation at 809 K and cooling in N_2. The initial 5×5 pattern (○) (coverage = 1.3 ML) is after many heating steps changed into the $(3\sqrt{3} \times 3\sqrt{3})R30^\circ$ pattern (◇) (coverage = 1.06 ML) and finally into the 3×3 pattern (△) (coverage = 0.54 ML).

surface under vacuum was never observed in the present experiments. Segregation experiments after saturation at 809 K, 200 or 500 Torr for 30 or 60 min, resulted in either a weak 1×1 LEED pattern with a bright background or the $(3\sqrt{3} \times 3\sqrt{3})R30^\circ$ or the 5×5 pattern depending on the segregation temperature (531, 624, and 670 K, respectively).

Finally it should be mentioned that another new structure was seen in one experiment. In this case the crystal with a very low level of bulk nitrogen was saturated under "normal" conditions (50 Torr nitrogen, 60 min at 809 K) and cooled down in nitrogen, which resulted in a coverage of 0.71 ML. The 6×6 LEED pattern obtained is shown in Fig. 8d. Due to the high nitrogen bulk diffusion rate at 809 K it is not possible within the exposure time to build up the high surface coverage required for forming the 5×5 structure. This is confirmed by the subsequent experiment. After the bulk was emptied and the surface was cleaned by sputtering, the crystal was again exposed to 50 Torr nitrogen for 60 min, this time at 670 K. A coverage of 0.93 ML and the 5×5 structure were obtained.

3.6. Temperature-Programmed Desorption

A TPD spectrum obtained after a 1.5×10^{-3} Torr exposure at 640 K for 20 min (nitrogen coverage ~0.6 ML) by heating the crystal from 440 to 948 K at a rate of 2 K/s is in Fig. 10 compared to a N_2 TPD spectrum from Ertl and coworkers (10) using 4×10^{-4} Torr exposure (coverage not reported). The agreement is satisfactory considering the differences in heating rate, exposures, and bulk desorption.

TPD spectra corresponding to the opposite extreme with respect to preexposure were also obtained. A TPD spectrum obtained after high exposures at 809 K by 500 Torr nitrogen and cooling down in nitrogen is shown in Fig. 11.

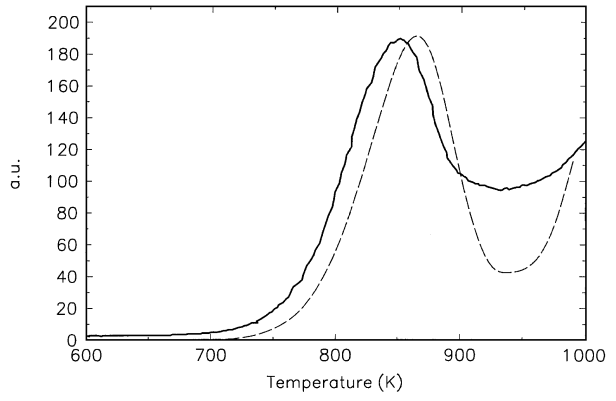

FIG. 10. N_2/Fe(111) TPD after 1.5×10^{-3} Torr, 20 min exposure at 640 K. Heating rate 2 K/s. For comparison a TPD spectrum from Ref. (10) is also shown (dashed).

One very sharp peak with an unusual shape is seen at about 848 K and a broader one is seen at 873 K. The unusual shape of the first peak suggests that it reflects a phase transition, e.g., a collapse of a surface reconstruction, when the coverage decreases below a critical value. The detailed history of the treatments of the crystal prior to the TPD spectrum of Fig. 11 is as follows: The crystal without nitrogen was exposed at 809 K to 500 Torr nitrogen for 4 h and cooled down in nitrogen after which a TPD experiment was conducted (not shown). The surface was then cleaned by argon ion sputtering and as before exposed to 500 Torr nitrogen for 1 h at 809 K and cooled down in nitrogen. XPS measurements showed that the coverage just before TPD was 1.10 ML. Isothermal desorption experiments were conducted in order to better characterize the surface state(s) by eliminating the temperature dependence of the desorption rate. After the crystal was exposed at 809 K to 50 Torr nitrogen for 60 min and cooled down in nitrogen the crystal was heated at the usual rate (2 K/s) from 440 to 809 K; i.e.,

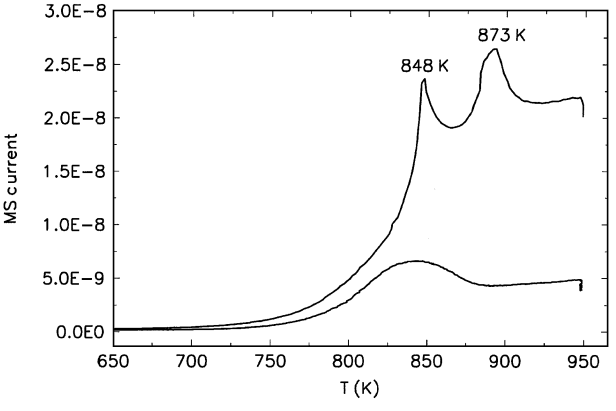

FIG. 11. N_2/Fe(111) TPD after 500 Torr, >4 h exposure at 809 K and cooling in N_2. Heating rate 2 K/s. For comparison the TPD spectrum from Fig. 10 is also shown.

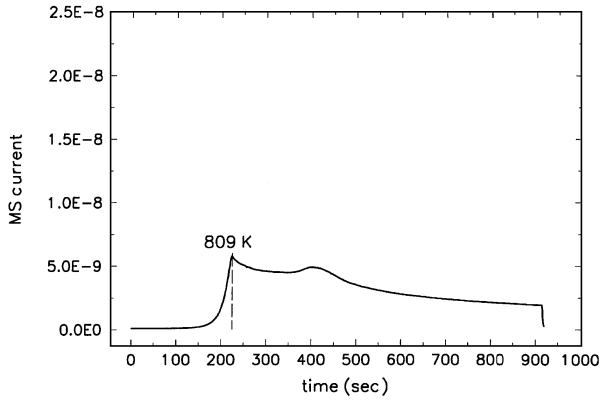

FIG. 12. Isothermal N_2 desorption at 809 K after 500 Torr, 60 min exposure at 809 K, cooling in N_2, and a linear temperature rise at 2 K/s from 440 to 809 K.

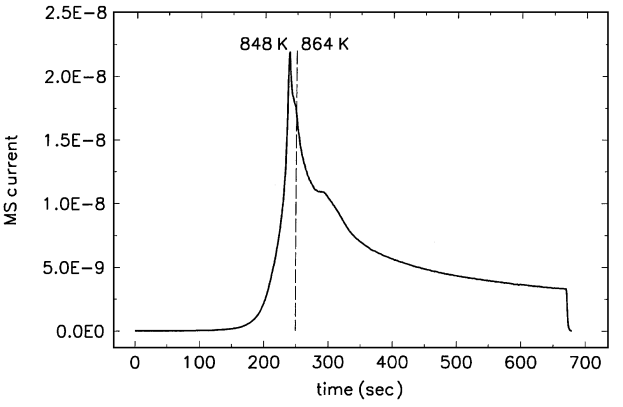

FIG. 13. Isothermal N_2 desorption at 864 K after 500 Torr, 60 min exposure at 809 K, cooling in N_2, and a linear temperature rise at 2 K/s from 440 to 864 K.

the rise was stopped before the first peak developed. Then the temperature was kept constant at 809 K for ca. 11 min. The nitrogen mass spectrometer (MS) current versus time is shown in Fig. 12. It is seen that after ca. 2 min the normal monotonous decrease of the desorption rate is interrupted by a peak, indicating that the structure becomes unstable when the coverage becomes smaller than a critical value. At this stage the coverage was reduced to 0.78 ML and LEED showed a change from the 5×5 to the $(3\sqrt{3} \times 3\sqrt{3})R30^\circ$ structure. A new combined TPD and isothermal desorption experiment was carried out without further exposure between the experiments to see if any trace of the first peak remained and if a breakdown of an unstable structure could still be observed during the isothermal desorption. In this case the crystal was heated linearly from 440 to 864 K, i.e., a temperature between the two peaks in Fig. 11, and kept at 864 K for ca. 5 min. In the TPD spectrum a very small, broad peak could just be seen above the strongly rising background due to the desorption of nitrogen from the bulk. No peak developed during the isothermal desorption at 864 K. The latter experiment was then repeated after exposing the crystal again at 809 K to 50 Torr nitrogen for 60 min and cooling down in nitrogen. The desorption rates measured as a function of time are shown in Fig. 13. As in Fig. 11 a sharp peak is seen at 848 K during the linear heating; 864 K was reached after 250 s and the temperature was then kept constant. It is seen that the monotonous decrease of the desorption rate was also in this case interrupted by a peak. The development of the peak started ca. 30 s after the start of the isothermal desorption at 864 K.

The TPD spectra obtained were, as mentioned above, strongly influenced not only by the temperature, pressure, and time used in the adsorption process prior to the TPD but also by the content of bulk nitrogen left from previous experiments. To investigate the dependence on the amount of nitrogen deposited in the crystal and at the same time to avoid the latter complication a series of TPD experiments was carried out, where prior to the experiment the bulk concentration of nitrogen was decreased to a very low level by isothermal desorption at 948 K until the rate of desorption became very small. In each experiment the crystal was, before linear heating from 440 to 948 K, exposed to 50 Torr nitrogen for 60 min at different temperatures in the range 485–809 K and cooled down in nitrogen. The TPD spectra obtained are shown in Fig. 14. It is seen that the spectra obtained using exposure temperatures in the range 578–763 K have two peaks which are growing and moving toward higher peak temperatures when the exposure temperature is increased. The spectra obtained after the lowest, 485 K, and the highest exposure temperature, 809 K, differ qualitatively from the other spectra in Fig. 14 by having one peak only. The total amount of nitrogen, N_{tot} deposited during the preexposure was determined by integrating the MS current for the TPD and for the isothermal desorption part of the experiment. The peak temperatures, the start coverages (from XPS peak area ratio), and N_{tot} are shown

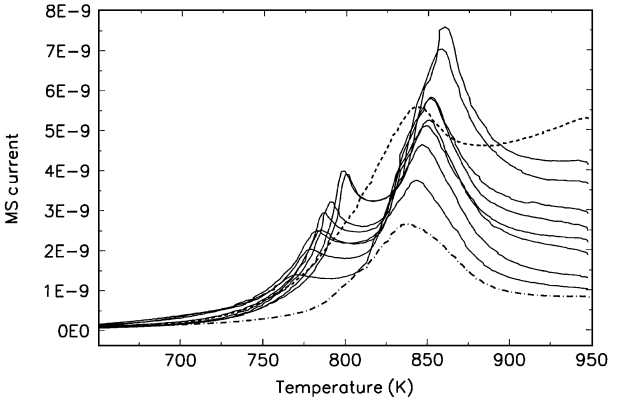

FIG. 14. N_2/Fe(111) TPD spectra obtained after 50 Torr, 1 h exposure at the following temperatures: 485 (- · · · -), 578, 624, 670, 693, 716, 763, and 809 K (- - -). Cooling in N_2. Heating rate 2 K/s.

TABLE 4

N_2/Fe(111) TPD after 1 h Exposure

Exposure: 50 Torr, 1 h, +TPD + isotherm desorption (948 K)					
T_{expos} (K)	Total desorption (ML)	Initial coverage (ML)	Calc. bulk (ML)	T_{p1} (K)	T_{p2} (K)
485	0.88	0.88	0.001	—	837
578	1.53	0.93	0.028	771	843
624	1.64	0.90	0.087	779	847
670	2.08	0.93	0.228	785	850
693	3.02	0.96	0.352	788	852
716	3.36	0.93	0.528	790	852
739	4.34	0.92	0.772	799	857
763	4.86	1.00	1.120	801	860
809	8.46	0.71	2.149	—	842

in Table 4. It is seen that coverages are almost the same for all the two-peak spectra while it is significantly lower for the two one-peak spectra. It is obviously not possible to obtain a coverage sufficiently high to form the two-peak state at the lowest exposure temperature. Neither is it possible at the highest temperature, 809 K, due to the high bulk diffusion rate preventing the surface concentration, to reach the critical coverage.

That the surface state of the crystal, as revealed by TPD spectra, depends sensitively on the history of the crystal is illustrated further in Fig. 15. Two TPD spectra, Nos. 1 and 2, obtained after our standard presaturation, 809 K, 500 Torr nitrogen, 1 h, cooling down in nitrogen and subsequent sputter cleaning and adsorption experiments, are shown together with the high-exposure spectrum from Fig. 11, denoted No. 3. The surface nitrogen coverage measured by XPS was almost the same for the three spectra: 1.04, 1.10, and 1.10 ML, respectively. After the standard presaturation and sputter cleaning but before TPD2 the surface was exposed at 485 K to 500 Torr nitrogen for 1 h. In the case of TPD1 three sputter cleaning and adsorption experiments were made after the standard presaturation but before TPD1. The first two adsorption experiments were made at 485 K, 1 Torr nitrogen in about 1 h, while the last one was done at 578 K, 500 Torr nitrogen in 1 h. Despite the fact that the adsorptions prior to the TPD were made at a higher temperature in TPD1 than in TPD2 the peak temperatures are higher in the latter spectrum. This is probably due to the larger number of sputter cleanings before TPD1 than before TPD2 removing more subsurface nitrogen in the former case. It is also seen in Fig. 15 that the peak corresponding to the second peak at 893 K in Fig. 11 is composed of at least two components in the TPD1 and TPD2 spectra at 870, 880 and 874, 887 K, respectively. Also the shape of the second peak in the spectra corresponding to exposure temperatures 716, 739, and 763 K in Fig. 14 shows that the peak is composed of more than one components.

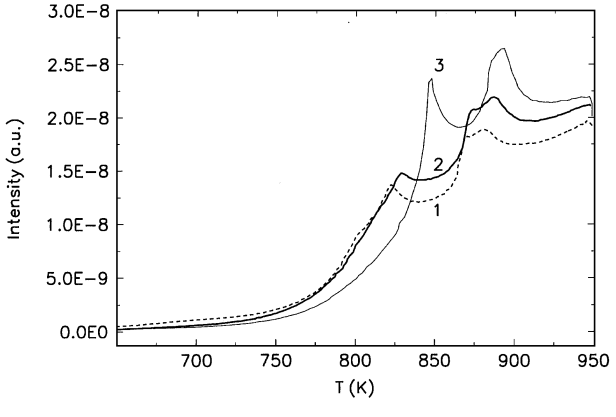

FIG. 15. Two N_2/Fe(111) TPD spectra, 1 and 2, obtained after 500 Torr, 1 h exposure at 809 K, cooling in N_2, and additional sputter cleaning plus N_2 adsorption. Heating rate 2 K/s. Spectrum 3 is the high-exposure spectrum shown in Fig. 11. Initial coverage is almost the same (∼1.1 ML) for the three spectra. Different adsorption temperatures and sputter cleanings (see text for details).

3.7. Correlation between Surface Structure and TPD Spectra

A number of TPD studies were carried out subsequent to surface structure characterization by LEED after different pretreatments. The results of such a series of TPD experiments (designated Nos. 57, 62 to 65, and 68) are illustrated in Table 5 and Fig. 16. In all cases, except experiment 63, the nitrogen concentration in the bulk was brought down to a very low level by desorption at 948 K before the indicated exposure. In experiment 63 the crystal was exposed to 500 Torr nitrogen at 809 K for 60 min and cooled down in nitrogen, then the surface was cleaned by Ar^+ ion sputtering, and finally it was exposed to 500 Torr nitrogen at 670 K for 60 min (and cooled down in nitrogen) as indicated in Table 5. By comparing the structure information in Table 5 and Fig. 16 it is seen that a 5×5 structure always results in a TPD spectrum with two peaks. TPD spectrum 64

TABLE 5

N_2/Fe(111) LEED and TPD after 1 h Exposure and Cooling in Nitrogen

T_{expos} (K)	N_2 pressure (Torr)	θ_i (ML)	θ_f (ML)	LEED structure	TPD No.
809	500	0.97	0.06	5×5	57
578	500	0.87	0.05	5×5, weak	62
670[a]	500	0.92	0.07	5×5	63
670	5	0.82	0.05	$(3\sqrt{3} \times 3\sqrt{3})$	64
670	100	0.88	0.04	5×5	65
670	500	0.92	0.04	5×5	68

[a] Prior to exposure the crystal was exposed at 809 K to 500 Torr nitrogen for 1 h and cooled down in nitrogen. The surface was subsequently cleaned by sputtering.

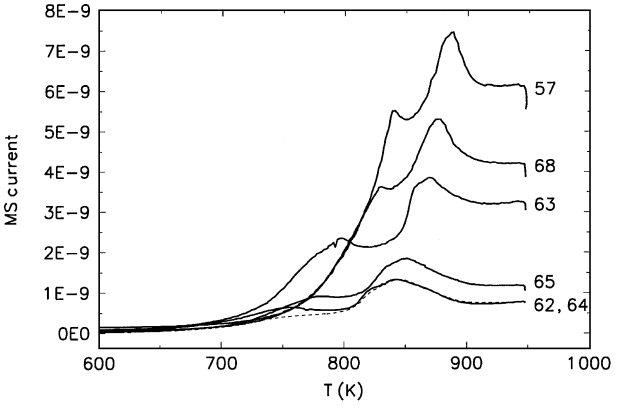

FIG. 16. N_2/Fe(111) TPD spectra obtained after formation of the 5×5 (Nos. 57, 62, 63, 65, and 68) and the $(3\sqrt{3} \times 3\sqrt{3})R30^\circ$ surface structure (No. 64).

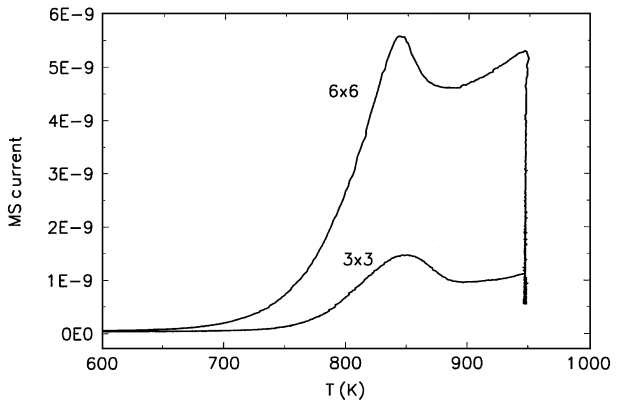

FIG. 18. N_2/Fe(111) TPD spectra obtained after formation of the 3×3 and 6×6 surface structures, respectively.

corresponding to the $(3\sqrt{3} \times 3\sqrt{3})R30^\circ$ structure is shown with a dashed line in Fig. 16. It is seen that it closely resembles spectrum 62 but the first peak has almost disappeared and the shoulder of the second peak is smaller. This is more clearly seen in Fig. 17. The 5×5 structure always gives TPD spectra with two peaks while the 3×3 and the 6×6 structures give only one TPD peak as illustrated in Fig. 18.

4. DISCUSSION

4.1. Adsorption Experiments

The motivation for undertaking a new study of the interaction of nitrogen with Fe(111), despite the apparent completeness of the previous studies by Ertl and co-workers, was, as mentioned in the Introduction, that it has been suggested (18, 19) that a possible explanation of the apparent inconsistency of the catalyst and the single-crystal adsorption results may be that the effective gas temperature was unknown but smaller than the surface temperature

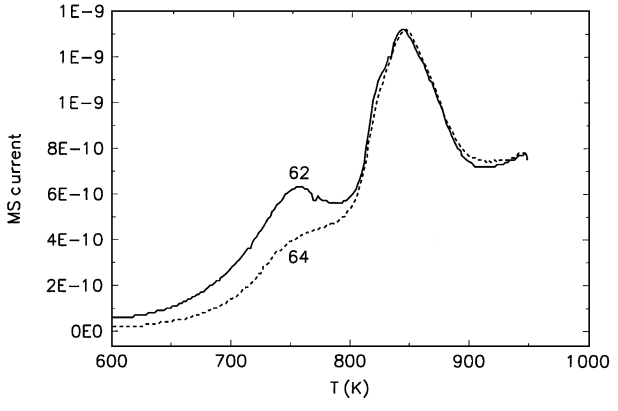

FIG. 17. Comparison of the N_2/Fe(111) TPD spectra 62 and 64 obtained after formation of the 5×5 and the $(3\sqrt{3} \times 3\sqrt{3})R30^\circ$ surface structure, respectively.

in the experiments of Ertl co-workers (10) because of the low pressure used. Therefore, in the present study adsorption measurements were performed after exposures made with pure nitrogen at low pressures and also using similar nitrogen partial pressures but much higher total pressures by adding argon. It turned out that all the adsorption measurements at the same temperature contributed within the accuracy of the measurements to one and the same adsorption curve independent of the total pressure. The conclusion is that the dissociative adsorption of nitrogen on Fe(111) depends very little on the gas temperature, at least in the temperature range covered by the present adsorption experiments, 393–578 K. How can this result agree with the strong energy dependence of the beam results of Rettner and Stein (16)?

First, it is very difficult to compare monoenergetic molecular beam results with results obtained by adsorption from an equilibrium environmental gas because an accurate extrapolation to low energies is required in order to derive a gas temperature-dependent sticking coefficient for a Maxwell–Boltzmann gas by integration over all molecular beam energies. Second, the result of Rettner and Stein (16) were obtained at a fixed surface temperature (520 K) while the environmental gas results correspond more closely to a gas temperature which is equal to (or lower than) the surface temperature. Rettner and Stein (16) investigated the influence of the surface temperature at one beam energy (1.05 eV). If we assume that this dependence applies also at the other beam energies and that normal energy scaling is a good approximation then the environmental nitrogen initial sticking coefficient can in principle be derived by integrating the beam results corrected for surface temperature change. Rettner and Stein (16) state that contributions of vibrationally excited molecules are small and need not be taken into account. The results of such calculations are shown in Fig. 19 together with the initial sticking coefficients from Table 1. The solid and the long-dashed lines represent results calculated without and with

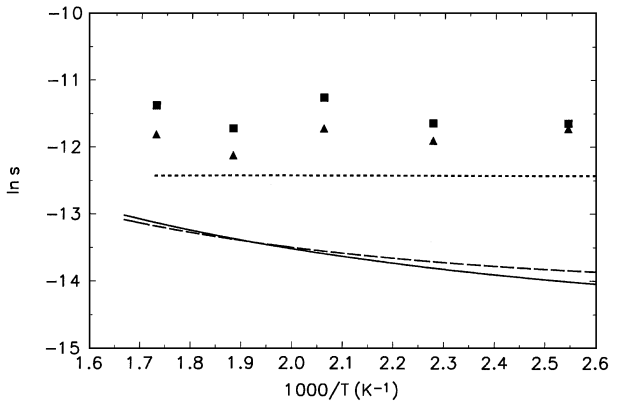

FIG. 19. Initial dissociative sticking coefficients for N_2 on Fe(111) from Table 1 compared with that obtained by Ertl and co-workers (2) (- - -) and with the Maxwell–Boltzmann gas sticking coefficients calculated from the molecular beam results of Rettner and Stein (16), not corrected (—) and corrected (– – –) for surface temperature dependence.

corrections for surface temperature dependence, respectively. The short-dashed line shows the value of the initial sticking coefficient as reported by Ertl and co-workers (2). The temperature dependence derived from the beam data is, in the temperature range of the present work, surprisingly weak corresponding to an average activation energy of about 7 kJ/mol in reasonable agreement with the lack of any significant temperature dependence of the initial sticking coefficients of the present work and Ertl and co-workers (2). It is seen in Fig. 19, however, that the absolute values of the initial sticking coefficients calculated from the beam results of Rettner and Stein (16) are about a factor of 7 smaller than those determined in the present work and about three times smaller than those obtained by Ertl and co-workers (2). The fact that the present results show, in agreement with Ertl and co-workers (10), that the temperature dependence of the initial sticking coefficient is negligible may be explained by a precursor mechanism as suggested by Ertl and co-workers (2) while the strong energy dependence of the beam results is more easily explained by a direct dissociation process. The fact that the integration of the beam results gives sticking coefficients much smaller than those measured in the experiments of Ertl and co-workers (10) and in the present work may then be explained by a change of dominating mechanism when going from low to high energies. Recently Hansen *et al.* (38) have performed dynamical calculations of the dissociative chemisorption of N_2 molecules on Fe(111) based on a semiempirical potential energy surface. In their model the collision time is much shorter than the oscillation period of the physisorbed molecule so they concluded that no precursor state is involved. They suggest that the decrease in sticking probability with increasing surface temperature observed by Rettner and Stein (16) is somehow caused by the interaction with substrate motion. Darling and Holloway (39) have criticized this suggestion. They point out that the surface mass model (39), which in the present case is a good approximation, cannot yield a decrease in sticking probability with increasing surface temperature for a rising dissociation curve. Beam studies by Rettner and Stein (40) show that vibrational excitation of the N_2 molecules of the beam enhances the dissociative sticking probability, indicating that not all the molecules are equilibrated in a precursor state before dissociation under the conditions of the beam experiment. This reinforces our suggestion that the dominating mechanism changes with increasing energy from a precursor to a direct process.

The coverage dependence of the dissociative sticking probability is probably closely related to the structure changes revealed by LEED. The saturation coverage of the adsorption curves (Table 1) increases by about 20% when increasing the adsorption temperature from 393 to 578 K. The results of Ertl and co-workers (10) show a much larger increase in the saturation coverage with increasing temperature, ca. 70% in the temperature range from 373 to 508 K. This difference may be due to the much higher pressures used in the present work when saturating the surface, causing the saturation level at the lower temperatures to come closer to the high-temperature saturation level. The fact that the coverage can be increased beyond the adsorption saturation level (~0.85 ML) to above 1 ML by segregation may be explained as a difference between dissociative molecular nitrogen adsorption and atomic nitrogen adsorption. In the former case three to four free sites are needed for dissociation to take place, while only one site is needed for atomic nitrogen adsorption.

4.2. Simulation of a Catalyst Experiment

Having confirmed the validity of the results of Ertl and co-workers (10) it remains to explain the surprisingly low rate of nitrogen adsorption on a singly promoted iron catalyst recently observed in a TPA experiment (17). The simulation of this catalyst TPA experiment using the Fe(111) crystal shows that an adsorption rate of the same low order of magnitude is measured for the crystal at 350 K as was obtained for the catalyst. In the case of the Fe(111) crystal the explanation is clear. A significant part of the molecules adsorbed at low temperature does not desorb during heating but is dissociated, giving a surface coverage of 0.65 ML at 350 K as measured by XPS. The final saturation coverage for nitrogen adsorption in Fe(111) is found to be about 0.8 ML for sufficient high exposures. However, it is seen in Fig. 4 and Table 1 that 0.7 ML corresponds to intermediate saturation with very low sticking probability at 393 K, respectively. An intermediate saturation at 0.5 ML has been seen in 300 K adsorption experiments. Therefore it is very plausible that 0.65 ML is close to such an intermediate saturation coverage at 350 K, explaining the very low

adsorption rate observed. We suggest that the same explanation applies to the catalyst, but note that it has not been proved because information about nitrogen coverages on the catalyst surface is lacking.

4.3. *LEED and TPD Experiments*

The most surprising result of the present study is the observation of new nitrogen chemisorption states formed at high exposures with temperatures above 570 K and elevated nitrogen pressure as revealed by TPD spectra and LEED patterns. For exposures at 50 Torr and temperatures in the range 570–760 K a new 5×5 surface structure is developed. This structure is also developed at 809 K if the bulk of the crystal contains significant amounts of nitrogen from previous experiments or if the pressure used during exposure is higher, e.g., 500 Torr. To our knowledge this structure has not been reported before in connection with nitrogen adsorption on Fe(111). However, it is interesting that Yoshida and Somorjai (41) reported on the observation of 5×5 structures in an exploratory LEED and AES investigation of surface structures formed when CO, CO_2, C_2H_2, C_2H_4, H_2, and NH_3 are chemisorbed on Fe(110) and Fe(111) surfaces. When C_2H_2 or C_2H_4 was adsorbed on the Fe(111) surface using an exposure $\gtrsim 1 \times 10^{-6}$ Torr × s a 3×3 structure was formed by heating to 600 K. This was changed into a 1×1 structure by further heating to 850 K. Also adsorption of CO and CO_2 resulted in 3×3 and 1×1 structures but in this case by heating to 720 and 800 K, respectively. After repeated exposures and flash desorption a 5×5 structure was formed by heating to 700 K after CO, CO_2, C_2H_2, or C_2H_4 was adsorbed. When the surface was heated to higher temperatures the 5×5 structure was changed into a 3×3 structure. When NH_3 was adsorbed at 270 K a streaky pattern was seen. On heating to 420 K it was converted into a 5×5 structure with streaks and then to a $(\sqrt{21} \times \sqrt{21})$R10.9° surface structure. Heating to 850 K produced a sharp 3×3 surface structure. Yoshida and Somorjai (41) presented a schematic diagram of the 5×5 LEED pattern formed after NH_3 adsorption. Most of the spots corresponding to a complete 5×5 structure are missing so it looks different from the 5×5 patterns seen in the present work. Only the spots nearest the 1×1 spots plus three more spots on top of small striations and closer to the (0, 0) spot are visible. We have been able to obtain a fully developed, sharp 5×5 structure by exposing the clean Fe(111) crystal to NH_3 at 670 K (42). The doser was not calibrated so the exposure is not known accurately, but is estimated to be lees than about 1000 ML, i.e., many orders of magnitude smaller than the exposures used in the N_2 adsorption experiments. It is well known that the same state of nitrogen in iron can be obtained at a far lower ammonia than nitrogen pressure when the hydrogen pressure is low. Ertl *et al.* (43) demonstrated this fact in the case of the formation of the Fe_4N nitride using the known thermodynamic expressions for the solubility of nitrogen in iron and the equilibrium between nitrogen in iron and in Fe_4N nitride together with the equilibrium constant for the ammonia synthesis reaction. They calculated, e.g., that at 670 K a nitrogen pressure of 3100 atm (1 atm = 101,325 Pa) is equivalent to an ammonia pressure of 3.6×10^{-11} atm for the formation of Fe_4N when the hydrogen pressure is 1×10^{-4} Torr. Yoshida and Somorjai (41) did not report the NH_3 exposure used in their work, and it is not clear whether several exposures and flash desorptions were needed for the formation of the 5×5 structure obtained by NH_3 adsorption. Anyhow, it is very probable that it is the same 5×5 surface structure, although perhaps incomplete, as the one seen in the present work. It may then by concluded that an equivalent surface structure can be obtained by adsorbing and decomposing carbon containing molecules on Fe(111).

The close link between the features of the TPD spectra and the LEED patterns allowed us to follow the transformation of the structure during isothermal desorption. The results on Fig. 12 show that the disappearance of the 5×5 structure during desorption is not gradual, but that the structure breaks down when the coverage is reduced to a certain critical value, somewhat higher than the coverage, 0.78 ML, in the end of the experiment of Fig. 12, where the $(3\sqrt{3} \times 3\sqrt{3})$R30° structure was observed. In the two subsequent experiments in which the temperature of the crystal was increased linearly with time of 864 K and then kept constant, the first without and the second with reexposure before the experiment, a peak was seen during the isothermal desorption only in the second experiment (Fig. 13). Although most of the first peak is desorbed during the temperature rise in the second experiment, making it plausible that the structural transformation $5 \times 5 \rightarrow (3\sqrt{3} \times 3\sqrt{3})$R30° has taken place, we cannot be absolutely sure that the transformation has been brought to completion and that the peak seen during the isothermal desorption shows that the $(3\sqrt{3} \times 3\sqrt{3})$R30° structure also breaks down when the coverage becomes smaller than a critical value. However, this assertion is supported by the results of some isothermal desorption experiments, which we have conducted (42), but do not discuss in any detail in the present paper. In some of them two peaks have been seen, e.g., during desorption at 763 and 739 K from initial coverage of 0.95 and 0.96 ML, respectively. Thus also the $(3\sqrt{3} \times 3\sqrt{3})$R30° structure breaks down rapidly when the surface coverage is reduced below a critical value. The step heating experiment depicted in Fig. 9 shows that the 5×5 structure is very stable at 670 K under vacuum but is rapidly changed into the $(3\sqrt{3} \times 3\sqrt{3})$R30° structure when the crystal is heated to 780 K under vacuum. The latter structure is on the other hand rapidly changed into the 3×3 structure when the temperature is increased to 820 K. From the fact that we have not observed the "intermediate" structures, $(\sqrt{19} \times \sqrt{19})$R23.4° and $(\sqrt{21} \times \sqrt{21})$R10.9°, we can only

conclude that they are transformed rapidly under the conditions of our experiments, but not that they are unstable also at other conditions.

At all the exposures giving TPD spectra with two peaks, e.g., all those in Fig. 14 corresponding to 50 Torr, 60 min exposure in the temperature range 578–763 K, for which LEED patterns have been obtained, a more or less well-developed 5×5 pattern is seen. However, when the exposure temperature is increased to 809 K, the high bulk diffusion rate prevents the build up of the 5×5 surface structure within the 60 min, 50 Torr exposure if the bulk initially has a very low concentration of nitrogen. In the only case in which a LEED observation was made after such an exposure, a 6×6 LEED pattern appeared, clearly different from the other patterns observed although the coverage measured (0.70 ML) is within the range (0.5–0.9 ML) where the $(3\sqrt{3} \times 3\sqrt{3})$R30° structure has been observed.

It may be suggested that the TPD, isothermal desorption, and LEED results may be explained by assuming that the 5×5 structure is a reconstruction which permits a higher number of nitrogen atoms to be incorporated in the surface. The reconstruction can only take place in the presence of a source of atomic nitrogen because the surface is inert to dissociative chemisorption of nitrogen before the formation of the 5×5 structure. In our case the atomic nitrogen is provided by the bulk through segregation. When the extra nitrogen incorporated in the 5×5 structure is removed from the surface then the reconstruction is lifted.

It is interesting to compare the total amount of nitrogen desorbed during the TPD plus isothermal desorption experiments of Fig. 14 to the amount of nitrogen diffused into the bulk during exposure plus the initial amount in the surface, i.e., the initial coverage. In Table 4 are shown the total amounts desorbed from one side of the crystal slab, the initial coverages, and the amounts diffused into the bulk of half of the crystal slab. The total amount desorbed is determined by integrating the mass spectrometer current during desorption and scale the value so that the amount is equal to the coverage at the lowest temperature (485 K) where the amount diffused into the bulk is negligible. The amount diffused into the bulk during exposure is calculated by numerical integration of the diffusion equation assuming a constant source equal to the solubility, $[N_\alpha]$, of nitrogen in α-iron (atomic ratio) (44)

$$[N_\alpha] = 5.01 \times 10^{-3} \exp(-32.5/RT) \times P_{N_2}^{1/2} \qquad [3]$$

and using the expression for the diffusion constant for nitrogen in iron given by da Silva and McLellan (45). In expression [3] the pressure is in atm and the activation energy in kJ/mol. At the higher temperatures the sum of the coverage and the amount diffused into the bulk is smaller than the total amount desorbed. However, excellent agreement is obtained, as shown in Fig. 20, if we amplify the strength of the diffusion source by a factor of 3.8. Edge contributions to the diffusion have not been taken into account in the calculation. For our crystal slab they may contribute up to 30% more bulk nitrogen, which may reduce the amplification factor to 2.7. It is probable that this deviation may be explained by uncertainties in the available diffusion and solubility data.

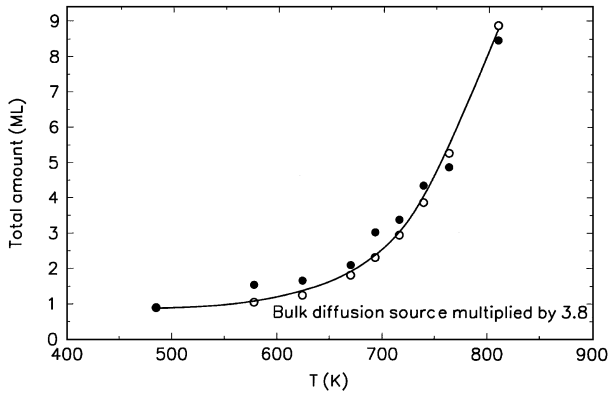

FIG. 20. Total N_2 amounts (●) desorbed during the TPD experiments of Fig. 14 and the sums of the initial coverage and the calculated amount deposited in the bulk multiplied by 3.8 (○).

4.4. The 5×5 Surface State and the Synthesis Reaction

In the course of the present studies we have unfortunately not been able to obtain the experimental information necessary for answering the crucial question, whether these new surface states are important for the understanding of the ammonia synthesis under industrial conditions. However, if we assume that the 5×5 state has an appreciable subsurface extension and that this means that bulk thermodynamics can be applied, then information about the nitridation potential, a_N, necessary for the formation of the 5×5 surface state may be extracted from the present experimental results. It is clear that the 5×5 surface state can be formed in the temperature range 570–765 K using a nitrogen pressure of 50 Torr. The equilibrium constant, K_{eq}, for the ammonia synthesis equilibrium

$$N_2 + 3H_2 \rightleftarrows 2NH_3 \qquad [4]$$

is given by

$$K_{eq} = \frac{P_{NH_3}^2 P_0^2}{P_{N_2} P_{H_2}^3}, \qquad [5]$$

where P_0 is the standard pressure (1 atm). By rearranging [5] the following expression for the nitridation potential, a_N, equivalent to pure nitrogen at the pressure P_{N_2} is obtained (where P_{N_2} is measured in atm):

$$a_N = \frac{P_{NH_3}}{P_{H_2}^{3/2}} = (K_{eq} P_{N_2})^{-1/2} \quad [\text{atm}^{-1/2}]. \qquad [6]$$

Nitridation potentials equivalent to 50 Torr nitrogen are in Table 6 compared to nitridation potentials for the effluent

TABLE 6

Nitridation Potential a_N of the Effluent Gas in NH_3 Synthesis Experiments

T (K)	Pressure (atm)	a_N of effluent gas ($atm^{-1/2}$)	Upper limit a_N of 5×5 ($atm^{-1/2}$)
763	214	0.031–0.023	0.0011
723	320–107	0.050–0.018	0.0017
683	320–107	0.041–0.015	0.0028
643	214	0.015	0.0050
623	214	0.010	0.0069
604	214	0.0047	0.0094
575	1	0.0036–0.0023	0.016
551	1	0.0025–0.0015	0.025
524	1	0.0015–0.00089	0.044

ammonia synthesis gas calculated from results obtained at temperatures in the range 604–763 K and pressures in the range 107–320 atm (46) and from results obtained in the temperature range 524–575 K at 1 atm (47). These two sets of experimental data are reproduced and compared to microkinetic models by Aparicio and Dumesic (48). It is seen in Table 6 that all the nitridation potentials of the effluent gas of the 1 atm experiments are much smaller than the potentials calculated for the 5×5 surface state. It is therefore very unlikely that the 5×5 state is present under the 1 atm reaction conditions. Conversely, it is tempting to conclude from the results in Table 6 that the 5×5 state is formed under high-pressure synthesis conditions. However, under real synthesis conditions the presence of hydrogen and significant amounts of hydrogen containing species, NH, NH_2, and NH_3, on the surface may reduce the probability for the formation of the 5×5 state. More detailed studies taking the coverage of these surface species into account must be carried out before a reliable conclusion can be reached. In the above-mentioned experiments, in which the 5×5 state was formed using low pressures of NH_3, it can be estimated that due to the very low hydrogen pressure the nitridation potential was orders of magnitude higher than the potentials in Table 6.

5. CONCLUSIONS

The present study of the interaction of nitrogen with the Fe(111) surface using partial and total pressures from 10^{-4} to 500 Torr and temperatures in the range 300–809 K leads to the following conclusions:

1. The dissociative chemisorption probability depends at small exposures very weakly on the gas temperature, indicating a precursor mechanism at thermal energies.

2. The adsorption saturation coverage increases weakly with temperature in the range 393–578 K from about 0.72 to 0.85 ML. However, the coverage (measured by XPS) can be increased further to about 1.1 ML by segregation, showing that more nitrogen can be incorporated in the surface from an atomic source than by dissociative chemisorption.

3. At high exposures, e.g., 50 Torr, 1 h, and temperatures in the range 570–765 K (or higher temperatures but also higher pressures), a new 5×5 surface structure is seen. A subsequent TPD spectrum contains two peaks, which moves to higher temperatures when the initial coverage is increased. At the lower coverage obtained by a 50 Torr, 1 h exposure at 809 K a 6×6 structure may appear. The corresponding TPD spectrum contains only one peak.

4. Peaks appearing during isothermal desorption experiments after formation of the 5×5 or the $(3\sqrt{3} \times 3\sqrt{3})R30^\circ$ surface structure show that these surface states break down when the coverage is reduced below critical values. During breakdown the 5×5 structure is transformed into the $(3\sqrt{3} \times 3\sqrt{3})R30^\circ$ surface structure.

5. Estimates made from the measured coverages and from the measured total amounts desorbed of the amounts of nitrogen deposited in the crystal in the combined TPD and isothermal desorption experiments after exposures at high temperatures (~700–800 K) are in reasonable agreement with the calculated amounts diffused into the crystal considering the uncertainties of the absolute values of the diffusion coefficient and solubility of nitrogen in iron.

6. Thermodynamic estimates show that the 5×5 surface state may be formed under industrial ammonia synthesis conditions on part of the surface, if the formation is not prevented by significant amounts of adsorbed hydrogen or hydrogen containing species.

ACKNOWLEDGMENTS

The authors benefited from discussions with L. M. Aparicio, J. A. Dumesic, B. Fastrup, M. Muhler, J. K. Nørskov, P. Stoltze, and E. Törnqvist. The authors thank J. H. Larsen and S. Christensen for assistance with some of the measurements. This work was supported by the Danish Research Councils through the Center for Surface Reactivity. The Center for Atomic-scale Materials Physics (CAMP) is sponsored by the Danish National Research Foundation.

REFERENCES

1. Ertl, G., *in* "Catalysis: Science and Technology" (J. R. Anderson and M. Boudart, Eds.), Vol. 4, p. 209. Springer-Verlag, Berlin, 1983.
2. Grunze, M., *in* "The Chemistry and Physics of Solid Surfaces and Heterogeneous Catalysis" (D. A. King and D. P. Woodruff, Eds.), Vol. 4, p. 413. Elsevier, Amsterdam, 1982.
3. Ertl, G., *Catal. Rev. Sci. Eng.* **21**, 201 (1980).
4. Ertl, G., *J. Vac. Sci. Technol. A* **1**, 1247 (1983).
5. Ertl, G., *CRC Crit. Rev. Solid State Mater. Sci.* **3**, 349 (1982).
6. Ertl, G., *in* "Catalytic Ammonia Synthesis, Fundamentals and Practice" (J. R. Jennings, Ed.), p. 109. Plenum Press, New York, 1991.
7. Stoltze, P., and Nørskov, J. K., *Phys. Rev. Lett.* **55**, 2502 (1985); *Surf. Sci.* **189/190**, 91 (1987); *Surf. Sci. Lett.* **197**, L230 (1988); *J. Catal.* **110**, 1 (1988).
8. Stoltze, P., *Phys. Scr.* **36**, 824 (1987).

9. Bowker, M., Parker, I. B., and Waugh, K. C., *Appl. Catal.* **14**, 101 (1985).
10. Bozso, F., Ertl, G., Grunze, M., and Weiss, M., *J. Catal.* **49**, 18 (1977).
11. Bozso, F., Ertl, G., and Weiss, M., *J. Catal.* **50**, 519 (1977).
12. Schlögl, R., *in* "Catalytic Ammonia Synthesis, Fundamentals and Practice" (J. R. Jennings, Ed.), p. 19. Plenum Press, New York, 1991.
13. Schütze, J., Mahdi, W., Herzog, B., and Schlögl, R., *Topics Catal.* **1**, 195 (1994).
14. Emmett, P. H., and Brunauer, S., *J. Am. Chem. Soc.* **56**, 35 (1934).
15. Scholten, J. J. F., Zwietering, P., Konvalinka, J. A., and de Boer, J. H., *Trans. Faraday Soc.* **55**, 2166 (1959).
16. Rettner, C. T., and Stein, H., *Phys. Rev. Lett.* **59**, 2768 (1987).
17. Fastrup, B., *J. Catal.* **150**, 345 (1994).
18. Bowker, M., *Catal. Today* **12**, 153 (1992).
19. Muhler, M., Rosowski, F., and Ertl, G., *Catal. Lett.* **24**, 317 (1994).
20. Schouten, F. C., Kaleveld, E. W., and Bootsma, G. A., *Surf. Sci.* **63**, 460 (1977).
21. Schouten, F. C., Gijzeman, O. L. J., and Bootsma, G. A., *Surf. Sci.* **87**, 1 (1979).
22. Beebe, T. B., Jr., Goodman, D. W., Kay, B. D., and Yates, J. T., Jr., *J. Chem. Phys.* **87**, 2305 (1987).
23. Chorkendorff, I., Alstrup, I., and Ullmann, S., *Surf. Sci.* **227**, 291 (1990).
24. Hanley, L., Xu, Z., and Yates, J. T., Jr., *Surf. Sci. Lett.* **248**, L265 (1991).
25. Nielsen, B. Ø., Luntz, A., Holmblad, P. M., and Chorkendorff, I., *Catal. Lett.* **32**, 15 (1995).
26. Shirley, D. A., *Phys. Rev. B* **5**, 4709 (1972).
27. Tougaard, S., *Surf. Sci.* **216**, 343 (1989).
28. Tokutaka, H., Ishihara, N., Nishimori, K., Kishida, S., and Isomoto, K., *Surf. Interface Anal.* **18**, 697 (1992).
29. Alstrup, I., Chorkendorff, I., and Ullmann, S., *Z. Phys. Chem. NF*, **198**, 123 (1997).
30. Alstrup, I., Chorkendorff, I., and Ullmann, S., *Surf. Sci.* **234**, 79 (1990).
31. Scofield, J. H. *J. Electron Spectrosc. Relat. Phenom.* **8**, 129 (1976).
32. Reilman, R. F., Msezane, A., and Manson, S. T., *J. Electron Spectrosc. Relat. Phenom.* **8**, 389 (1976).
33. Castle, J. E., and West, R. H., *J. Electron Spectrosc. Relat. Phenom.* **19**, 409 (1980).
34. Lee, S. B., Weiss, M., and Ertl, G., *Surf. Sci.* **108**, 357 (1981).
35. Müller, O. G., Kätzel, W., and Storbeck, F., *Phys. Status Solidi A* **89**, 89 (1985).
36. Legg, K. O., Jona, F., Jepsen, D. W., and Marcus, P. M., *Surf. Sci.* **66**, 25 (1977).
37. Whitman, L. J., Bartosch, C. E., and Ho, W., *J. Chem. Phys.* **85**, 3688 (1986).
38. Hansen, F. Y., Henriksen, N. E., and Billing, G. D., *Surf. Sci.* **324**, 55 (1995).
39. Darling, G. R., and Holloway, S., *Rep. Prog. Phys.* **58**, 1595 (1995).
40. Rettner, C. T., and Stein, H., *J. Chem. Phys.* **87**, 770 (1987).
41. Yoshida, K., and Somorjai, G. A., *Surf. Sci.* **75**, 46 (1978).
42. Alstrup, I., Chorkendorff, I., and Ullmann, S., unpublished.
43. Ertl, G., Huber, M., and Thiele, N., *Z. Naturforsch. A* **34**, 30 (1979).
44. Kubaschewski, O., "Iron—Binary Phase Diagrams." Springer-Verlag, Berlin, 1982.
45. da Silva, J. R. G., and McLellan, R. B., *Mater. Sci. Eng.* **26**, 83 (1976).
46. A. Nielsen, "An Investigation on Promoted Iron Catalysts for the Synthesis of Ammonia." Gjellerup, Copenhagen, 1967.
47. Ozaki, A., Taylor, H., and Boudart, M., *Proc. Roy. Soc. A* **258**, 47 (1960).
48. Aparicio, L. M., and Dumesic, J. A., *Topics Catal.* **1**, 233 (1994).